TABLE 3.7 Actinic Flux Values $F(\lambda)$ at the Earth's Surface as a Function of Wavelength Interval and Solar Zenith Angle within Specific Wavelength Intervals for Best Estimate Surface Albedo Calculated by Madronich (1998)[a]

Wavelength interval (nm)	Exponent[b]	Solar zenith angle (deg)									
		0	10	20	30	40	50	60	70	78	86
		Actinic fluxes (photons cm^{-2} s^{-1})									
290–292	14	0.00	0.00	0.00	0.00	0.00	0.00	0.00	0.00	0.00	0.00
292–294	14	0.00	0.00	0.00	0.00	0.00	0.00	0.00	0.00	0.00	0.00
294–296	14	0.00	0.00	0.00	0.00	0.00	0.00	0.00	0.00	0.00	0.00
296–298	14	0.01	0.01	0.01	0.01	0.00	0.00	0.00	0.00	0.00	0.00
298–300	14	0.03	0.03	0.02	0.02	0.01	0.00	0.00	0.00	0.00	0.00
300–302	14	0.07	0.07	0.06	0.04	0.03	0.01	0.00	0.00	0.00	0.00
302–304	14	0.18	0.18	0.15	0.12	0.08	0.04	0.01	0.00	0.00	0.00
304–306	14	0.33	0.32	0.29	0.23	0.16	0.09	0.04	0.01	0.00	0.00
306–308	14	0.51	0.49	0.45	0.37	0.28	0.17	0.08	0.02	0.00	0.00
308–310	14	0.66	0.65	0.60	0.51	0.40	0.27	0.14	0.04	0.01	0.00
310–312	14	0.99	0.97	0.90	0.79	0.64	0.45	0.25	0.09	0.02	0.00
312–314	14	1.22	1.19	1.12	1.00	0.82	0.61	0.36	0.14	0.04	0.00
314–316	14	1.37	1.34	1.27	1.14	0.96	0.73	0.46	0.20	0.06	0.01
316–318	14	1.67	1.64	1.56	1.42	1.22	0.95	0.62	0.29	0.10	0.01
318–320	14	1.70	1.68	1.60	1.47	1.27	1.01	0.69	0.34	0.13	0.02
320–325	14	5.30	5.24	5.03	4.66	4.10	3.34	2.36	1.27	0.52	0.10
325–330	14	7.72	7.63	7.36	6.88	6.15	5.12	3.75	2.15	0.96	0.22
330–335	14	8.26	8.17	7.91	7.44	6.70	5.65	4.23	2.50	1.16	0.29
335–340	14	7.98	7.91	7.67	7.24	6.56	5.59	4.25	2.58	1.23	0.33
340–345	14	8.64	8.57	8.32	7.88	7.17	6.15	4.73	2.91	1.40	0.38
345–350	14	8.73	8.65	8.42	7.99	7.30	6.30	4.88	3.04	1.47	0.40
350–355	14	10.00	9.92	9.67	9.20	8.43	7.31	5.71	3.60	1.76	0.47
355–360	14	8.98	8.91	8.69	8.28	7.62	6.64	5.22	3.33	1.64	0.43
360–365	14	9.97	9.90	9.67	9.23	8.52	7.46	5.91	3.80	1.88	0.49
365–370	15	1.24	1.23	1.20	1.15	1.07	0.94	0.75	0.48	0.24	0.06
370–375	15	1.10	1.09	1.07	1.02	0.95	0.84	0.67	0.44	0.22	0.06
375–380	15	1.26	1.25	1.22	1.17	1.09	0.97	0.78	0.52	0.26	0.07
380–385	15	1.06	1.06	1.04	1.00	0.93	0.82	0.67	0.45	0.23	0.06
385–390	15	1.17	1.16	1.14	1.10	1.03	0.92	0.75	0.50	0.26	0.06
390–395	15	1.17	1.17	1.14	1.10	1.03	0.92	0.76	0.51	0.27	0.07
395–400	15	1.43	1.42	1.40	1.35	1.26	1.13	0.93	0.64	0.33	0.08
400–405	15	2.02	2.01	1.98	1.91	1.79	1.61	1.33	0.91	0.48	0.12
405–410	15	1.97	1.96	1.92	1.86	1.75	1.57	1.30	0.90	0.48	0.12
410–415	15	2.06	2.04	2.01	1.94	1.83	1.65	1.37	0.96	0.51	0.12
415–420	15	2.09	2.08	2.05	1.98	1.87	1.69	1.41	0.99	0.54	0.13
420–430	15	4.13	4.11	4.04	3.92	3.70	3.36	2.82	2.00	1.09	0.26
430–440	15	4.26	4.24	4.18	4.05	3.84	3.50	2.96	2.12	1.17	0.28
440–450	15	5.05	5.03	4.96	4.82	4.57	4.18	3.56	2.58	1.45	0.34
450–460	15	5.66	5.64	5.56	5.39	5.12	4.67	3.98	2.90	1.65	0.38
460–470	15	5.75	5.72	5.64	5.48	5.21	4.77	4.08	3.00	1.72	0.39
470–480	15	5.86	5.83	5.75	5.60	5.32	4.89	4.19	3.10	1.80	0.41
480–490	15	5.74	5.72	5.64	5.49	5.23	4.81	4.14	3.08	1.80	0.40
490–500	15	5.94	5.91	5.83	5.68	5.42	5.00	4.31	3.22	1.90	0.42
500–510	15	6.10	6.07	5.99	5.82	5.54	5.09	4.38	3.27	1.92	0.42
510–520	15	5.98	5.95	5.87	5.71	5.44	5.00	4.32	3.24	1.92	0.41
520–530	15	6.20	6.17	6.09	5.92	5.64	5.20	4.49	3.37	2.00	0.42
530–540	15	6.38	6.38	6.27	6.10	5.81	5.35	4.63	3.48	2.07	0.42
540–550	15	6.37	6.34	6.26	6.10	5.81	5.35	4.63	3.49	2.08	0.42
550–560	15	6.55	6.52	6.43	6.26	5.96	5.49	4.74	3.57	2.13	0.43
560–570	15	6.61	6.58	6.49	6.31	6.01	5.53	4.78	3.59	2.13	0.41
570–580	15	6.69	6.66	6.57	6.39	6.09	5.60	4.84	3.64	2.17	0.41
580–600	16	1.35	1.34	1.32	1.29	1.23	1.13	0.98	0.74	0.45	0.09
600–620	16	1.36	1.35	1.34	1.30	1.24	1.14	0.99	0.75	0.46	0.09
620–640	16	1.37	1.37	1.35	1.31	1.26	1.16	1.01	0.78	0.48	0.10
640–660	16	1.38	1.37	1.35	1.32	1.26	1.17	1.02	0.79	0.50	0.11
660–680	16	1.43	1.42	1.40	1.37	1.31	1.21	1.06	0.83	0.53	0.12
680–700	16	1.40	1.40	1.38	1.34	1.28	1.19	1.05	0.82	0.54	0.12

[a] The authors are grateful to Dr. Sasha Madronich for generously providing these calculations.

[b] This column lists the power of 10 by which all entries should be multiplied. For example, at $\theta = 0°$ the total actinic flux in the wavelength interval from 306 to 308 nm is 0.51×10^{14} photons cm^{-2} s^{-1}.

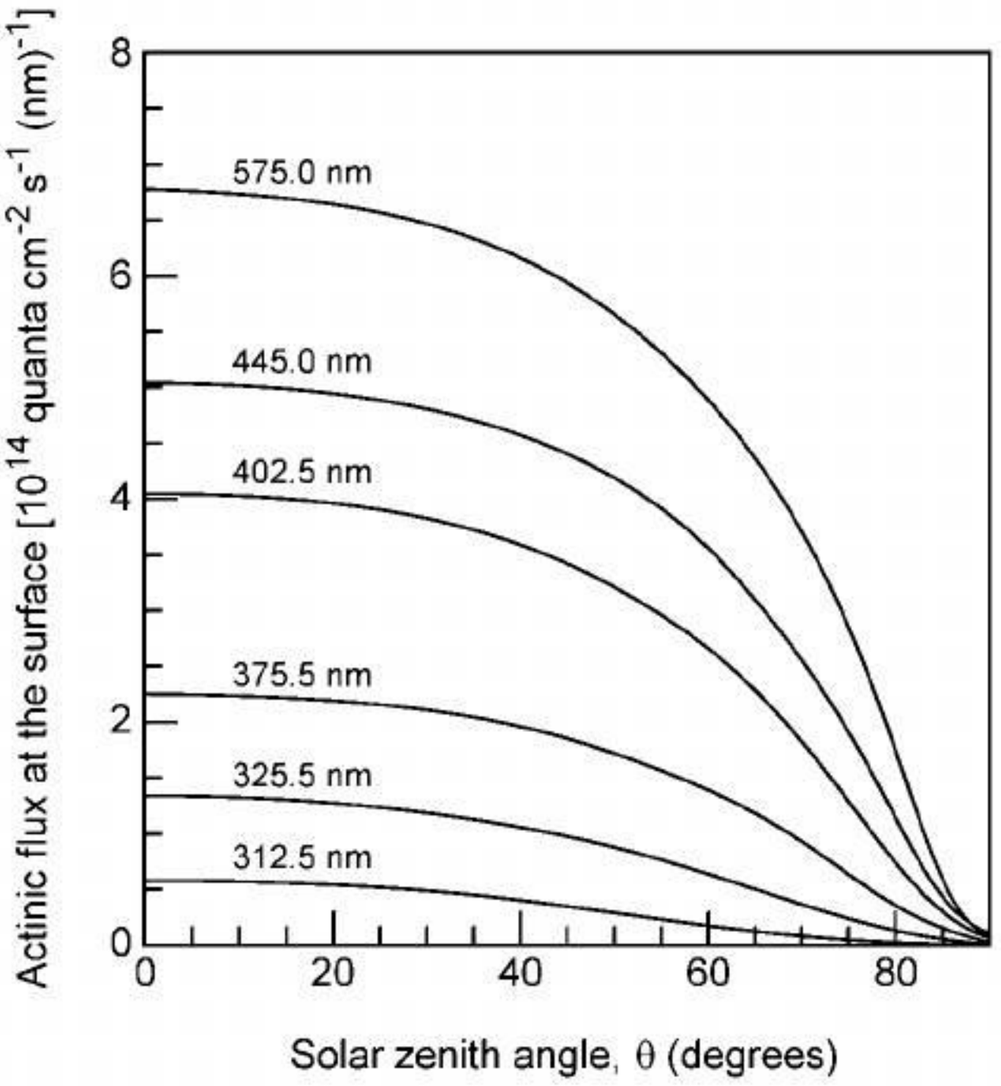

FIGURE 3.21 Calculated actinic flux centered on the indicated wavelengths at the earth's surface using best estimate albedos as a function of solar zenith angle (from Madronich, 1998).

concentrations were the same but that the Rayleigh scattering was reduced due to the lowered pressure, i.e., lower gas concentrations. The increase in actinic flux in the UV is relatively small ($< 5\%$) for zenith angles less than $\sim 45°$; at larger zenith angles, the change is less than 13%. For the longer wavelengths, it is small at all zenith angles. (Although these data are those of Peterson (1976) and Demerjian *et al.* (1980), since they are relative values, they are not expected to differ significantly from those that would be derived with the Madronich (1998) actinic flux values.)

TABLE 3.8 Correction Factors for Extraterrestrial Solar Flux Values Depending on Earth – Sun Distance at Various Times of the Year

Date	Correction factor	Date	Correction factor
Jan 1	1.033	Jul 1	0.966
Jan 15	1.032	Jul 15	0.967
Feb 1	1.029	Aug 1	0.970
Feb 15	1.024	Aug 15	0.974
Mar 1	1.018	Sep 1	0.982
Mar 15	1.011	Sep 15	0.989
Apr 1	1.001	Oct 1	0.998
Apr 15	0.993	Oct 15	1.006
May 1	0.984	Nov 1	1.015
May 15	0.978	Nov 15	1.022
Jun 1	0.971	Dec 1	1.027
Jun 15	0.968	Dec 15	1.031

Source: Demerjian *et al.* (1980).

e. Effect of Height above Earth's Surface on $F(\lambda)$

Figure 3.24 shows the *relative* changes in the total actinic flux as a function of altitude from 0 to 15 km at solar zenith angles of 20, 50, and 78° and at wavelengths of 332.5 (part a), 412.5 (part b), and 575 nm (part c), respectively. Again, since these are relative changes, these results of Peterson (1976) and Demerjian *et al.* (1980) are not expected to be significantly different from those that would be obtained with the Madronich (1998) actinic flux estimates.

At the largest solar zenith angle shown, 78°, all of the curves show a decrease in the actinic flux from 15 km to lower altitudes. This occurs because at these large values of θ and hence long path lengths through the atmosphere, backscattering of the light increases as it passes through the atmosphere.

The calculated actinic flux typically increases significantly in the first few kilometers. This is partly due to scattering of light by particulate matter and to light absorption by tropospheric O_3 close to the surface. The effect of O_3 can be seen by comparing the total fluxes at 332.5 nm (Fig. 3.24a), where O_3 absorbs, to those at 575 nm (Fig. 3.24b), where it does not.

Peterson and co-workers have examined the percentage increase in total actinic flux, going from the surface to ~ 1 km; they estimate that at short wavelengths ($\lambda \leq 310$ nm), the increase is $> 37.5\%$ for all zenith angles. This increase in flux with altitude at short wavelengths could be particularly significant in photochemical smog formation. Thus pollutants trapped in an inversion layer aloft may be exposed to higher actinic fluxes than at ground level and photolyze more rapidly, hastening the formation of various secondary pollutants. The increased actinic flux with altitude close to the earth's surface is the basis for their suggestion that the presence of increased O_3 in, or close to, the inversion layer may be at least partially the result of the height dependence of $F(\lambda)$.

These predictions have been borne out experimentally in studies in which the rate of photolysis of NO_2 was measured from the surface to ~ 7.6-km altitude and found to increase with height by more than 50% (Kelley *et al.*, 1995; Volz-Thomas *et al.*, 1996).

f. Sensitivity of Calculated Actinic Fluxes to Input Values for Surface Albedo and Ozone and Particle Concentrations

As discussed earlier, the net actinic flux incident on a volume of air is sensitive to a number of parameters,

TABLE 3.9 Tabulation of Solar Zenith Angles (deg) as a Function of True Solar Time and Month

	0400	0430	0500	0530	0600	0630	0700	0730	0800	0830	0900	0930	1000	1030	1100	1130	1200
								Latitude 20°N									
Jan 1							84.9	78.7	72.7	66.1	61.5	56.5	52.1	48.3	45.5	43.6	43.0
Feb 1						88.9	82.5	75.8	69.6	63.3	57.7	52.2	47.4	43.1	40.0	37.8	37.2
Mar 1						85.7	78.8	72.0	65.2	58.6	52.3	46.2	40.5	35.5	31.4	28.6	27.7
Apr 1					88.5	81.5	74.4	67.4	60.3	53.4	46.5	39.7	33.2	26.9	21.3	17.2	15.5
May 1					85.0	78.2	71.2	64.3	57.2	50.2	43.2	36.1	29.1	26.1	15.2	8.8	5.0
Jun 1				89.2	82.7	76.0	69.3	62.5	55.7	48.8	41.9	35.0	28.1	21.1	14.2	7.3	2.0
Jul 1				88.8	82.3	75.7	69.1	62.3	55.5	48.7	41.8	35.0	28.1	21.2	14.3	7.7	3.1
Aug 1					83.8	77.1	70.2	63.3	56.4	49.4	42.4	35.4	28.3	21.3	14.3	7.3	1.9
Sep 1					87.2	80.2	73.2	66.1	59.1	52.1	45.1	38.1	31.3	24.7	18.6	13.7	11.6
Oct 1						84.1	77.1	70.2	63.3	56.5	49.9	43.5	37.5	32.0	27.4	24.3	23.1
Nov 1						87.8	81.3	74.5	68.3	61.8	56.0	50.2	45.3	40.7	37.4	35.1	34.4
Dec 1							84.3	78.0	71.8	66.1	60.5	55.6	50.9	47.2	44.2	42.4	41.8
								Latitude 30°N									
Jan 1							89.4	83.7	78.3	73.2	68.4	64.1	60.4	57.3	55.0	53.5	53.0
Feb 1							86.2	80.3	74.6	69.1	64.1	59.4	55.3	51.9	49.3	47.7	47.2
Mar 1						87.5	81.1	74.9	68.8	62.9	57.4	52.2	47.5	43.5	40.3	38.4	37.7
Apr 1					87.2	81.4	74.9	68.5	62.1	55.8	49.6	43.8	38.2	33.3	29.3	26.5	25.5
May 1			88.9	82.7	76.3	69.9	63.4	56.9	50.4	44.0	37.6	31.4	25.6	20.4	16.5	15.0	
Jun 1			85.3	79.2	73.1	66.8	60.4	54.0	47.5	41.0	34.5	28.1	21.7	15.7	10.5	8.0	
Jul 1			84.7	78.7	72.5	66.3	60.0	53.5	47.1	40.6	34.1	27.7	21.2	15.1	9.6	6.9	
Aug 1			87.2	81.0	74.7	68.3	61.9	55.4	48.9	42.4	36.0	29.7	23.6	18.1	13.7	11.9	
Sep 1				85.9	79.4	72.9	66.4	60.0	53.6	47.3	41.2	35.5	30.2	25.8	22.8	21.6	
Oct 1					85.1	78.7	72.4	66.2	60.1	54.4	48.8	43.8	39.5	36.1	33.9	33.1	
Nov 1						84.6	78.4	72.8	67.1	62.0	57.0	53.0	49.3	46.7	44.9	44.4	
Dec 1						88.7	82.8	77.3	72.2	67.3	63.0	59.2	56.0	53.7	52.2	51.8	
								Latitude 40°N									
Jan 1							89.0	84.2	79.8	75.7	72.1	69.0	66.4	64.6	63.4	63.0	
Feb 1							84.8	79.8	75.2	70.7	67.0	63.5	60.9	58.8	57.6	57.2	
Mar 1						89.1	83.7	78.1	72.8	67.8	63.1	58.8	55.1	51.9	49.6	48.1	47.7
Apr 1						87.1	81.4	75.6	70.0	64.4	59.0	53.8	49.0	44.6	40.9	38.0	36.2	35.5
May 1					85.9	80.5	74.7	68.9	63.2	57.5	51.8	46.3	41.0	36.1	31.7	28.2	25.8	25.0
Jun 1				86.8	81.5	76.1	70.5	64.9	59.2	53.4	47.7	42.0	36.5	31.2	26.2	22.1	19.1	18.0
Jul 1				86.0	80.8	75.4	69.9	64.3	58.6	52.8	47.1	41.4	35.8	30.4	25.4	21.1	18.0	16.9
Aug 1				89.3	83.9	78.4	72.8	67.1	61.4	55.6	49.9	44.4	39.0	33.8	29.2	25.4	22.8	21.9
Sep 1					84.6	78.9	73.2	67.5	61.8	56.3	51.0	46.0	41.4	37.5	34.4	32.3	31.6	
Oct 1						86.3	80.6	75.1	69.7	64.5	59.6	55.1	51.2	47.8	45.3	43.6	43.1	
Nov 1							88.1	82.6	77.8	72.8	68.6	64.4	61.1	58.2	56.1	54.7	54.4	
Dec 1								88.1	83.3	78.8	74.7	71.0	67.8	65.3	63.3	62.2	61.8	
								Latitude 50°N									
Jan 1										86.5	83.2	80.2	77.7	75.7	74.2	73.3	73.0	
Feb 1								89.5	85.3	81.5	78.0	74.9	72.2	70.0	68.5	67.5	67.2	
Mar 1							86.3	81.8	77.4	73.3	69.6	66.2	63.2	60.9	59.1	58.0	57.7	
Apr 1						86.6	81.8	76.9	72.2	67.6	63.2	59.1	55.4	52.0	49.3	47.2	45.9	45.5
May 1				87.8	83.2	78.5	73.7	68.9	64.1	59.4	54.7	50.3	46.2	42.5	39.4	37.0	35.5	35.0
Jun 1			86.7	82.4	78.0	73.3	68.6	63.8	59.0	54.2	49.5	44.9	40.6	36.6	33.1	30.4	28.6	28.0
Jul 1	89.7		85.7	81.5	77.1	72.5	67.8	63.0	58.2	53.4	48.7	44.1	39.7	35.6	32.1	29.3	27.5	26.9
Aug 1			89.7	85.4	80.8	76.2	71.4	66.6	61.8	57.0	52.4	47.9	43.7	39.9	36.6	34.1	32.5	31.9
Sep 1					88.3	83.6	78.8	74.0	69.2	64.6	60.1	55.9	52.0	48.5	45.7	43.5	42.1	41.6
Oct 1							87.6	82.8	78.2	73.8	69.6	65.7	62.1	59.1	56.5	54.7	53.5	53.1
Nov 1									87.1	83.0	79.0	75.5	72.3	69.5	67.3	65.7	64.7	64.4
Dec 1									89.2	85.5	82.1	79.1	76.5	74.5	73.0	72.1	71.8	

Source: Peterson (1976) and Demerjian *et al.* (1980).